

Gait Characterization in Duchenne Muscular Dystrophy (DMD) Using a Single-Sensor Accelerometer: Classical Machine Learning and Deep Learning Approaches

Albara Ah Ramli^a, Huanle Zhang^a, Jiahui Hou^b, Rex Liu^a, Xin Liu^a, Alina Nicoricic^c, Daniel Aranki^d, Corey Owens^c, Poonam Prasad^c, Craig McDonald^c and Erik Henricson^{c,*}

^aDepartment of Computer Science, School of Engineering; University of California, Davis

^bDepartment of Electrical and Computer Engineering, School of Engineering; University of Waterloo, Ontario

^cDepartment of Physical Medicine and Rehabilitation, School of Medicine; University of California, Davis

^dDepartment of Electrical Engineering and Computer Sciences, School of Engineering; University of California, Berkeley

ARTICLE INFO

Keywords:

Duchenne Muscular Dystrophy (DMD)
Typically Developing (TD)
Artificial Intelligence (AI)
Deep Learning (DL)
Classical Machine Learning (CML)
Clinical Gait Feature (CF)
Time Window (TW)

Declarations of interest: none

ABSTRACT

Differences in gait patterns of children with Duchenne muscular dystrophy (DMD) and typically developing (TD) peers are visible to the eye, but quantification of those differences outside of the gait laboratory has been elusive. We measured vertical, mediolateral, and anteroposterior acceleration using a waist-worn iPhone accelerometer during ambulation across a typical range of velocities. Six TD and six DMD children from 3-15 years of age underwent seven walking/running tasks, including five 25m walk/run tests at a slow walk to running speeds, a 6-minute walk test (6MWT), and a 100-meter-run/walk (100MRW). We extracted temporospatial clinical gait features (CFs) and applied multiple Artificial Intelligence (AI) tools to differentiate between DMD and TD control children using extracted features and raw data. Extracted CFs showed reduced step length and a greater mediolateral component of total power (TP) consistent with shorter strides and Trendelenberg-like gait commonly observed in DMD. AI methods using CFs and raw data varied in effectiveness at differentiating between DMD and TD controls at different speeds, with an accuracy of some methods exceeding 91%. We demonstrate that by using AI tools with accelerometer data from a consumer-level smartphone, we can identify DMD gait disturbance in toddlers to early teens.

1. Introduction

Patterns of gait disturbance in boys with Duchenne muscular dystrophy (DMD) demonstrate biomechanical compensatory substitution to overcome strength loss and progressive joint contractures, and disease progression yields temporal and spatial changes in gait analysis metrics as described by Sutherland [28], D'Angelo [7], Heberer [13], and Gaudreault [11]. Perturbations and compensatory adaptations in gait are present from the onset of walking, are progressive, and follow a predictable pattern, with increasing anterior pelvic tilt, increasing foot internal rotation and decreasing hip extension in stance phase with lateral trunk lean toward the supporting limb, and increased hip flexion and hip abduction and decreased ankle dorsiflexion in the swing phase [28] [13] [11] [5]. The center of pressure at foot contact shifts laterally and anteriorly until an equinus posture at foot strike predominates [28]. These progressive limitations lead to decreased step length and cadence during ambulation, decreased relative power of anteroposterior movement, and increased relative power of mediolateral movement with concomitant impairment of gait velocity.

Recent advancements in novel muscle-sparing therapeutics highlight the desirability of initiating early disease modifying treatment in the toddler years, but relatively few re-

liable tools exist for quantitative measurement of strength, function, and mobility in this age group, underscoring an urgent need to develop new tools that include that age group and extend upward to the limits of ambulation [5]. Wearable accelerometers can accurately measure variation in step rates in children with DMD in both the laboratory and community settings, produce natural history data that is suitable for analysis in clinical trials [8], and hold promise to provide a complete picture of the effect of strength limitation on community mobility and daily activities. To maximize their effectiveness, wearable devices will need to detect and record well-understood quantitative temporal and spatial features of gait, and yet be unobtrusive and low-cost.

The increasing availability of high-quality, low-cost tri-axial accelerometers and inertial measurement units as stand-alone devices or integrated into commonly-available smartphones yields new opportunities to gather community level data across a wide range of typically-developing individuals and those affected by movement-related disorders. Because of this, researchers are developing a better understanding of how to extract and interpret temporal and spatial features of single accelerometer data that include step counts and frequencies but also a wide variety of other features [4] [16] including step lengths, step velocities [11] [29] and triaxial power spectra [14] [27] and to use those features in principal component analyses to evaluate between-group differences and changes over time [21]. The utility of these measures in describing disease severity and tracking disease progression has been demonstrated in the GRMD dog model of DMD

*Corresponding author

✉ ehenricson@ucdavis.edu (E. Henricson)

ORCID(s): 0000-0002-4617-225X (A.A. Ramli); 0000-0002-7511-6441 (E. Henricson)

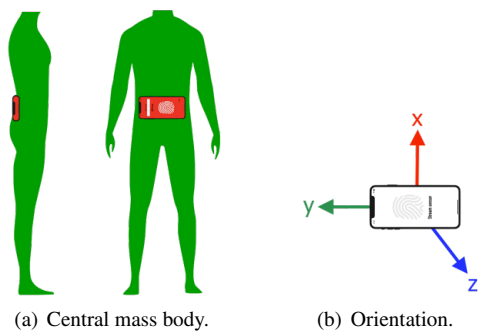


Figure 1: (a) The accelerometer records acceleration in the three axes of space represented in the right) is the right is the (full-back photograph), on the left is the (side photograph). The accelerometer is positioned on the center of the mass body and maintained by a belt fastened around the hip. (b) y-axis is mediolateral, the z-axis is anteroposterior, the x-axis is vertical. The accelerometer is a built-in chip in a smartphone.

[3], as well as in children with DMD [10].

In this project, we evaluate the utility of various classical machine learning (CML) and deep learning (DL)-based approaches to differentiate between children with and without DMD using data from consumer-level mobile phone accelerometers during walking and running tasks. We developed a system consisting of a smartphone-based software application to collect raw data remotely using the phone's built-in accelerometer sensor, combined with a web-based tool to aggregate, store and analyze data. We extracted the temporal/spatial gait characteristics and used CML and DL techniques [17] to evaluate the gait changes associated with DMD, using both extracted features and raw data.

2. Materials and Methods

2.1. Participants

The University of California, Davis institutional review board (IRB) reviewed and approved the protocol. Informed consent was obtained for each participant prior to initiation of study procedures. We studied twelve male participants (6 with DMD, 6 TD) who were between the ages of 3 and 15 years old, had at least 6 months of walking experience, and could perform a 10-meter run/walk test in less than 10 seconds. Participants with DMD had a confirmed clinical diagnosis and were glucocorticoid therapy-naïve or on a stable regimen for at least three months. North Star Ambulatory Assessment (NSAA) scores for DMD participants ranged from 31 to 13 indicating clinically-apparent mild to moderate mobility limitation (Table-1). Scores for TD children ranged from 34 to 31, indicating a maximal range of task performance, with a low score of 31 in the three-year-old participant indicating age-appropriate achievement of developmental milestones [6].

2.2. Materials

Participants wore an NGN Sport fitness phone belt (Engine Design Group, LLC, Los Angeles CA) carrying an Ap-

Table 1

Characteristic of the children included in the study.

ID	Case (status)	Age (years)	Weight (kg)	Height (cm)	NSAA Score (/34)
1	TD	11	38.4	147.6	34
2	TD	3	20	106.3	31
3	TD	11	44.5	144	34
4	TD	12	57.7	155.6	34
5	TD	5	20.3	119.3	34
6	TD	9	41.8	132.9	34
7	DMD	5	34.7	127	31
8	DMD	12	52.6	145	29
9	DMD	10	38.5	124.5	26
10	DMD	15	63.7	153.3	15
11	DMD	7	29.8	133	13
12	DMD	5	22.9	111.8	30

ple iPhone 11 (Apple, Inc. Cupertino CA), which includes a single built-in triaxial accelerometer. The belt was placed close to the body's center of mass at the lumbosacral junction at the approximate level of the iliac crest, with the phone oriented so that the right lower side was consistently oriented in the upper right position to measure acceleration in the vertical, mediolateral and anteroposterior axes (Fig-1(a)). The measurement range of the accelerometer was $\pm 2g$ with a resolution of 0.001g. We developed a smartphone app (Walk4Me) [25] [24] to continuously stream raw sensor data to a cloud server at a sampling rate of 30 Hz. At the conclusion of each assessment session, data was processed via a separate web-based Walk4Me application to extract clinical gait features and train the CML and DL models.

2.3. Gait Testing and Data Collection

Children performed a series of seven walking and running tasks along a 25m straight-line course as previously described [19]. The first five activities were speed-calibration-tests (SC) where the child walked along a 25m long corridor in an incrementally increasing gait velocity from slowest speed, speed-calibration-L1 (SC-L1), to a slow walk (SC-L2), to a comfortable self-selected pace (SC-L3), to a fast walk (SC-L4), to a run or fastest possible gait (SC-L5) [11], which could include running. The evaluator recorded the observed number of steps taken during each effort. Participants then performed a 6-minute walk test (6MWT), followed by a 100m run/walk using previously described methods [19] [1]. The evaluator recorded the 6-minute walk distance and number of steps in the first 50m, and time to complete the 100m run/walk. All evaluations were recorded on video for later verification of step counts, distances and task times.

2.4. Data Analysis

Data analysis was performed using multiple approaches (Fig-2). In our first approach, we processed raw data from each task to extract clinical gait features including speed, step length, step frequency, total power, percent of power in each axis, and force index in a manner similar to those

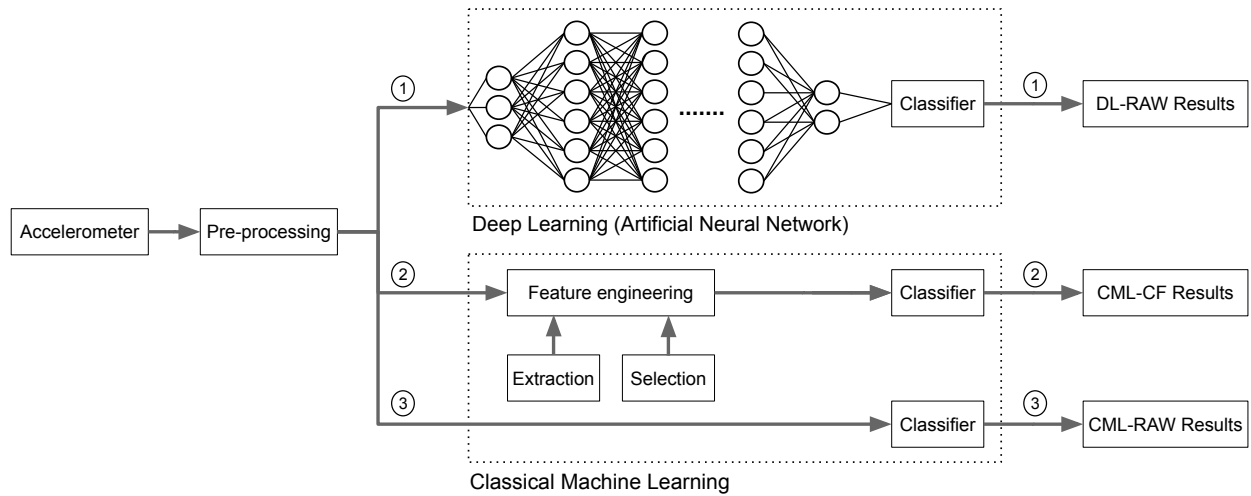


Figure 2: A typical process diagram of classical machine learning (CML) and deep learning (DL) of the three methods used: (1) DL-RAW, (2) CML-RAW, and (3) CML-CF.

described by Barthelemy [3] and Fraysse [9]. We normalized speed and step length to height. We compared means of features between DMD and TD control groups for each task using simple two-tailed T-tests. We evaluated differences in slopes of features across the range of velocities using STATA XT MIXED (multilevel mixed-effects linear regression) model repeated measures tools, accounting for repeated measures within participants. We then applied CML approaches to the clinical feature data both with and without dimensional reduction, and replicated those approaches using raw sensor data to identify data characteristics and models that were most accurate at predicting group membership.

2.4.1. Extraction and Evaluation of Clinical Gait Features

We extracted eight temporospatial clinical characteristics from the raw accelerometer data, including:

- **Speed (SP)** is measured in meters per second and normalized by the height of the child in meters. This feature is calculated by dividing the distance by the time spent performing each activity. Speed value has to be calculated, and we use a regression model to predict it. For each subject, we train a model using SC-L1 to SC-L5, which have fixed distances, we impute distances for all activities based on that model [15]. The ground-truth fixed distance of (SC-L1, SC-L2, SC-L3, SC-L4, SC-L5) were used to train the model. To evaluate our distance model accuracy, we compare our measured distance with the ground-truth distance.
- **Step Length (SL)** is measured in meters and normalized by the height of the child in meters. This feature is calculated by dividing the total distance by the number of steps. The number of steps was obtained by processing the anteroposterior signal of accelerometer (z-axis). Fig-4(c) and Fig-4(f) shows the accelerometer raw signal of a child with DMD and a TD child.

This total distance was calculated using a regression model that was built for each child from their SC (L1 to L5).

- **Step Frequency (SF)** is measured in steps per second. This feature is calculated by dividing the number of steps by time for each activity. The number of steps is calculated using a low pass filter on the anteroposterior (z-axis) acceleration signal (Fig-4(c) and Fig-4(f)). Then, we calculate the number of peaks, where each peak represents one step, and a complete gait cycle is composed of two steps.
- **Total Power (TP)** is measured in W/kg. This feature is calculated by first transferring the time domain to the frequency domain of the three axes: mediolateral (y-axis) Fig-4(e), anteroposterior (z-axis) Fig-4(f), and vertical (x-axis) Fig-4(d). Then, we sum the integral of the power (normalized by weight) in each of the three axes (Fig-4(h), Fig-4(i), and Fig-4(g)).
- **Mediolateral Power (MP)** is measured in % of TP. This feature is calculated by first transferring the time domain of the accelerometer's y-axis (Fig-4(e)) to the frequency domain using Fast Fourier Transform (FFT). Then we calculate the integral of the power spectrum (Fig-4(h)). Finally, we normalize the value by the weight and TP.
- **Anteroposterior Power (AP)** is measured in % of TP. This feature is calculated by first transferring the time domain of the accelerometer's z-axis (Fig-4(f)) to the frequency domain using FFT. Then we calculate the integral of the power spectrum density (PSD) (Fig-4(i)). Finally, we normalize the value by the weight and TP.
- **Vertical Power (VP)** is measured in % of TP. This feature is calculated by first transferring the time domain of the accelerometer's x-axis (Fig-4(d)) to the

Table 2

Summary of clinical features. SP: speed in meters per second normalized by height in meters. TP: total Power with unit of $\times 10^{-6}$ W/kg. SF: Step Frequency with a unit of step/sec. SL: Step length as a percentage of standing height. MP: the percentage of power in the x-axis normalized by total power VP: (%). AP: the percentage of power in the y-axis normalized by total power MP: (%). VP: the percentage of power in the z-axis normalized by total power AP: (%). FI: force index with unit of $\times 10^{-3}$ N/kg. The level of significance was set at $p = 0.05$. NS: p values that are not significant (< 0.05).

Activity	Case		SP	SF	SL (%)	TP ($\times 10^{-6}$)	VP (%)	MP (%)	AP (%)	FI ($\times 10^{-3}$)	(VP-AP) (%)
SC-L1	TD	Mean	0.35	1.32	0.26	72.79	31.16	36.77	32.07	23.93	-0.91
		(SD)	(0.07)	(0.13)	(0.03)	(79.91)	(5.03)	(8)	(6.63)	(28.13)	(8.63)
		DMD	Mean	0.27	1.12	0.24	45.53	36.14	32.78	31.08	7.68
		(SD)	(0.06)	(0.21)	(0.03)	(47.33)	(11.71)	(8.99)	(7.52)	(6.73)	(17.51)
		p value	NS	NS	NS	NS	NS	NS	NS	NS	NS
SC-L2	TD	Mean	0.58	1.71	0.33	210.81	33.36	36.7	29.94	25.46	3.43
		(SD)	(0.11)	(0.19)	(0.03)	(238.59)	(4.72)	(5.21)	(4.45)	(30.38)	(7.56)
		DMD	Mean	0.5	1.59	0.32	123.95	35.14	29.4	35.46	10.14
		(SD)	(0.09)	(0.15)	(0.04)	(71.68)	(8.93)	(6.69)	(6.53)	(7.64)	(14.14)
		p value	NS	NS	NS	NS	NS	NS	NS	NS	NS
SC-L3	TD	Mean	0.89	2.2	0.41	779.58	39.7	34.99	25.31	56.49	14.39
		(SD)	(0.21)	(0.49)	(0.03)	(1044.28)	(9.86)	(9.41)	(2.48)	(94.42)	(10.87)
		DMD	Mean	0.8	2.11	0.38	414.54	32.58	35.94	31.48	21.75
		(SD)	(0.17)	(0.24)	(0.04)	(259.21)	(5.74)	(5.08)	(2.8)	(17.63)	(7.46)
		p value	NS	NS	NS	NS	NS	NS	0.002	NS	0.0332
SC-L4	TD	Mean	1.11	2.45	0.45	1900.05	38.02	43.01	18.97	102.47	19.05
		(SD)	(0.18)	(0.36)	(0.04)	(1976.52)	(20)	(25.69)	(6.33)	(156.66)	(14.84)
		DMD	Mean	1.05	2.49	0.42	1463.23	24.99	49.99	25.01	46.49
		(SD)	(0.26)	(0.4)	(801.67)	(6.8)	(10.16)	(6.25)	(27.9)	(8.21)	
		p value	NS	NS	NS	NS	NS	NS	NS	NS	0.0203
SC-L5	TD	Mean	1.52	2.97	0.51	7124.66	37.71	40.51	21.78	185.79	15.92
		(SD)	(0.45)	(0.58)	(0.06)	(8176.64)	(14.02)	(17.13)	(4.77)	(316.54)	(12.06)
		DMD	Mean	1.28	2.68	0.47	3361.3	26.26	48.09	25.66	70.72
		(SD)	(0.45)	(0.5)	(2854.13)	(12.03)	(14.97)	(6.64)	(53.95)	(12.39)	
		p value	NS	NS	NS	NS	NS	NS	NS	NS	0.068
6MWT	TD	Mean	1.05	2.32	0.45	915.13	45.77	31.88	22.34	750.96	23.43
		(SD)	(0.13)	(0.19)	(0.04)	(612.32)	(8.42)	(9.56)	(2.84)	(539.89)	(8.15)
		DMD	Mean	0.78	2.09	0.37	705.78	35.87	33.27	30.86	579
		(SD)	(0.29)	(0.45)	(0.06)	(1094.77)	(6.73)	(6.06)	(4.03)	(750.88)	(9.29)
		p value	NS	NS	0.015	NS	0.049	NS	0.002	NS	0.0045
100MRW	TD	Mean	1.43	2.81	0.51	7304.77	42.73	40.58	16.69	770.69	26.04
		(SD)	(0.45)	(0.75)	(0.06)	(5260.62)	(17.1)	(18.27)	(1.3)	(1017.03)	(15.95)
		DMD	Mean	1.06	2.38	0.43	3293.61	31.16	44.36	24.48	318.74
		(SD)	(0.42)	(0.64)	(0.08)	(3389.67)	(12.01)	(14.93)	(5.08)	(187.84)	(10.82)
		p value	NS	NS	NS	NS	NS	NS	0.012	NS	0.0337
All	TD	Mean	0.99	2.26	0.42	2615.4	38.35	37.78	23.87	273.69	14.48
		(SD)	(0.47)	(0.68)	(0.09)	(4600.89)	(12.54)	(14.24)	(6.7)	(527.4)	(14.19)
		DMD	Mean	0.81	2.05	0.37	1294.79	31.87	38.9	29.23	152.59
		(SD)	(0.41)	(0.63)	(0.09)	(2058.07)	(9.65)	(12.06)	(6.56)	(343.56)	(11.27)
		p value	NS	NS	0.019	NS	0.01	NS	0.0004	NS	0.0001

frequency domain using FFT. Then we calculate the integral of the PSD (Fig-4(g)). Finally, we normalize the value by the weight and TP.

- **Force Index (FI)** is measured in N/kg. This feature

is calculated by first transferring the time domain of the accelerometer's z-axis (Fig-4(f)) to the frequency domain using FFT. Then, we divide the integral of the PSD (Fig-4(i)) by the average speed in order to aver-

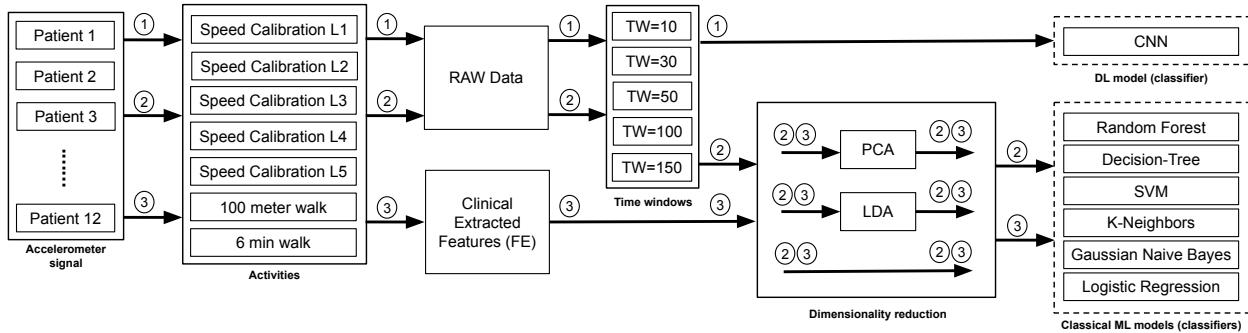


Figure 3: Fig: Process diagram of the three methods used: (1) DL-RAW, (2) CML-RAW, and (3) CML-CF.

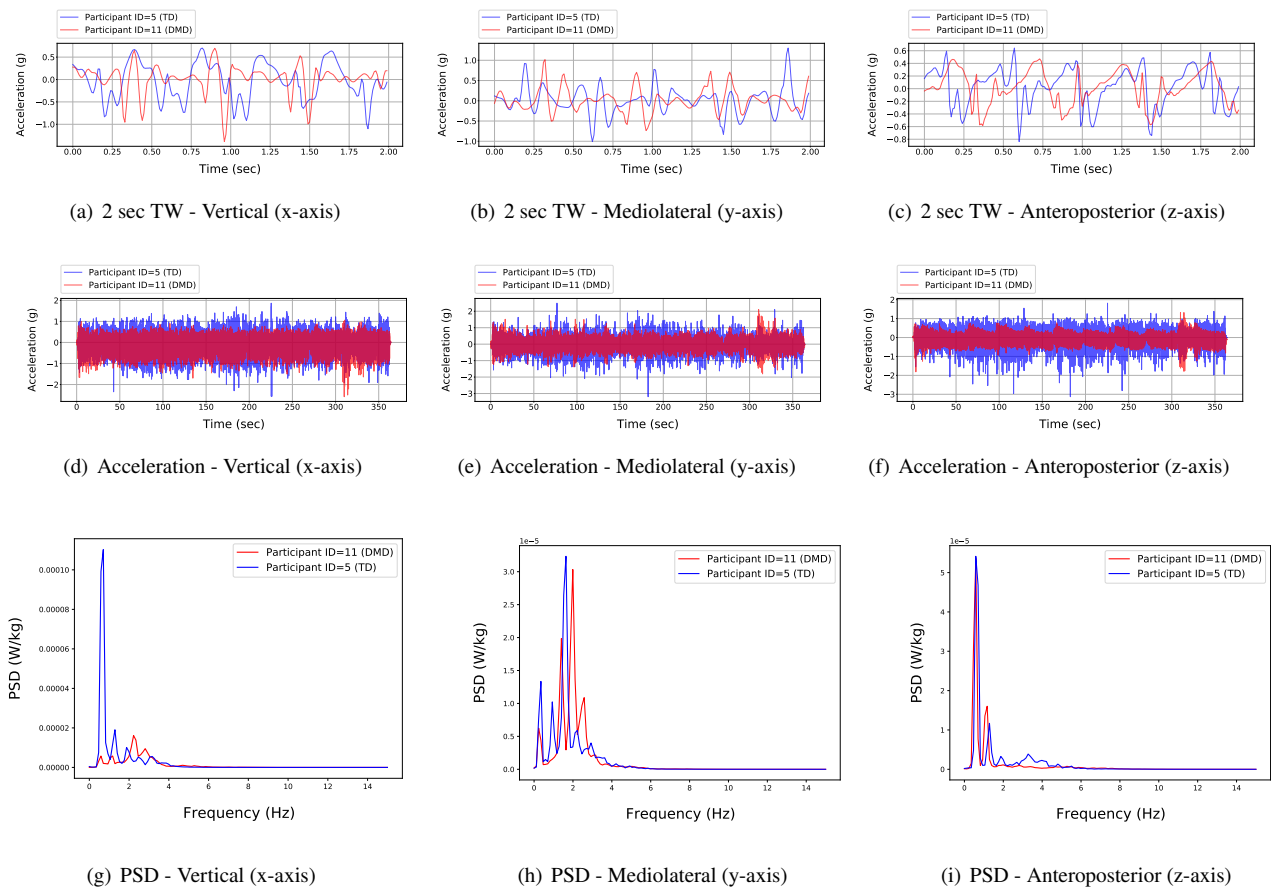


Figure 4: These figures illustrate a comparison of two children DMD (ID=11) and TD (ID=5), in the three-axial accelerations of 6MWT; (a, b, and c) represent a 2 sec TW of a TD child performs 5 steps, and a DMD child performs 4 steps. (d, e, and f) represent the TD child and the DMD child perform the whole 6MWT. (g, h, and i) represent Power-Spectrum-Density (PSD).

age the force index.

2.4.2. Dimensionality Reduction

To analyze how the participants are distributed on the projection plane, we used Principal Component Analysis (PCA) and Linear Discriminant Analysis (LDA) [2] [9]. We investigated whether using PCA and LDA techniques would affect the discrimination accuracy between DMD and TD groups. We fed the eight extracted CFs to CML models us-

ing PCA and LDA. We used PCA and LDA to reduce the dimensionality of the input feature of all participants and project their models' results into a two-dimensional (2D) and one-dimensional (1D) representation, respectively. We compared PCA and LDA accuracy with the original model without using any dimensionality reduction techniques (Fig-3).

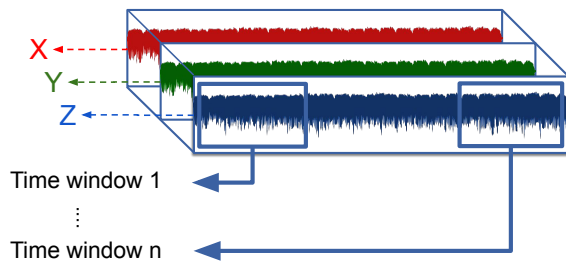


Figure 5: Time windows (TWs) of the accelerometer (x , y , and z axes)

2.4.3. Preprocessing of Raw Accelerometer Signals Using Time Windowing

In the CML-CF method, data from each activity for each participant represents an individual input to the model. The CFs of each activity must be extracted entirely before using it as an input to the model. In both the CML-RAW and DL-RAW methods we used raw acceleration values in each of the 3 axes of travel as an input to the CML and DL models (Fig-3). For CML with raw data (CML-RAW), we used the time-windowed raw data as an input to several classifiers with and without dimensionality reduction in a manner similar to our approach to analysis of extracted clinical features. For DL with raw data (DL-RAW) we used the time-windowed raw data as an input to a Convolutional Neural Network (CNN) [23] [26]. We limited pre-processing of raw data to segregating data from each task into multiple fixed time windows (TWs) (Fig-5) [18] to facilitate DL model convergence. We examined six distinct TWs (e.g., 0.3, 1, 1.6, 3, 3.3, 5 sec) to determine the signal duration required for the highest model accuracy to differentiate between data from people with DMD and TD controls. The data is collected at 30 Hz (where each second contain 30 samples). For each activity, the model predicts whether an individual TW is labeled as DMD or TD. We then used those predictions to calculate the overall percentage of the TWs that were predicted as DMD or TD. We set the threshold at 50% to determine if the participants were correctly labeled as having DMD.

2.4.4. Classical Machine Learning and Deep Learning Analytical Methods

We used three different AI models to evaluate optimal methods to classify accelerometer data collected at a range of gait speeds as belonging to a child with DMD or a TD control. For **CML-CF** method, 6 different classifiers were implemented: Random Forest (RF), Decision-Tree (DT), Support-Vector Machine (SVM), k-Nearest Neighbors (kNN), Gaussian Naive Bayes (GNB), Logistic Regression (LR). In this method, we used the eight extracted CFs as an input into CML classifiers with and without DR. The eight extracted CFs for each child were used to train the machine learning model for all seven activities. For **CML-RAW** method, we implemented the same 6 classifiers using time-windowed raw accelerometer signals as input features to the CML clas-

sifiers with and without dimensionality reduction. In both the CML-CF and CML-RAW approaches, we performed PCA and LDA separately for each gait activity to visualize TD and DMD children's variance between and within their groups. We plot their projection on a 1D and 2D planes. For the **DL-RAW** method, we used a CNN model with the time-windowed raw accelerometer signal as a feature in the DL classifier.

2.4.5. Cross-Validation of Artificial Intelligence Models

We used Leave-One-Out (LOO) cross-validation to calculate classification accuracy in the presence of slight variations in dataset contents. In LOO cross-validation, we train each model with the training set, and then we predict the test set. The present dataset contained 12 participants. We used data from 11 participants (92%) for the training-set to predict the group membership of the remaining 1 participant (8%), and repeated the analysis 12 times to obtain a model-based prediction for each participant. We calculated the accuracy of each model by averaging the 12-fold accuracy.

3. Results

3.1. Characteristics of Extracted Clinical Features

Group characteristics of clinical features extracted from sensor data during different activities and velocities are displayed in Table-2. Across all features and velocities, there was a trend whereby TD participants had higher mean values than their DMD counterparts, with the exception of the overall percentage of total power attributed to mediolateral movement, which was decreased. Step length was reduced in DMD participants compared to TD controls for the 6MWT (-8%), and for all efforts combined (-5%).

3.2. Changes in Power and Force With Increasing Speed

As the speed of ambulation increased, TP increased on a log scale in children with DMD and similar aged TD controls (Fig-6(d)). Range of TP was similar in both groups, but the slope of change with increasing velocity differed between groups ($p=0.012$) with the highest values in the DMD group being reached at lower velocities. In the TD control group, power increased with increasing speed of ambulation, with the highest velocities and powers being achieved by the older participants Fig-6(d). In the DMD group, power also increased with increasing speed of ambulation, but in this case the relationship with age was less clear. Some of the highest velocities and powers were achieved by the younger participants and stratification by age at a given unit speed was less apparent.

3.3. Changes in Axial Percentages of Total Power

Percentage of total power expended in vertical (VP), mediolateral (MP), and anteroposterior (AP) axes (Fig-6(a), Fig-6(b), and Fig-6(c)) also varied during ambulation from slow walk to running velocities, and patterns differed between children with DMD and TD controls. In typically developing

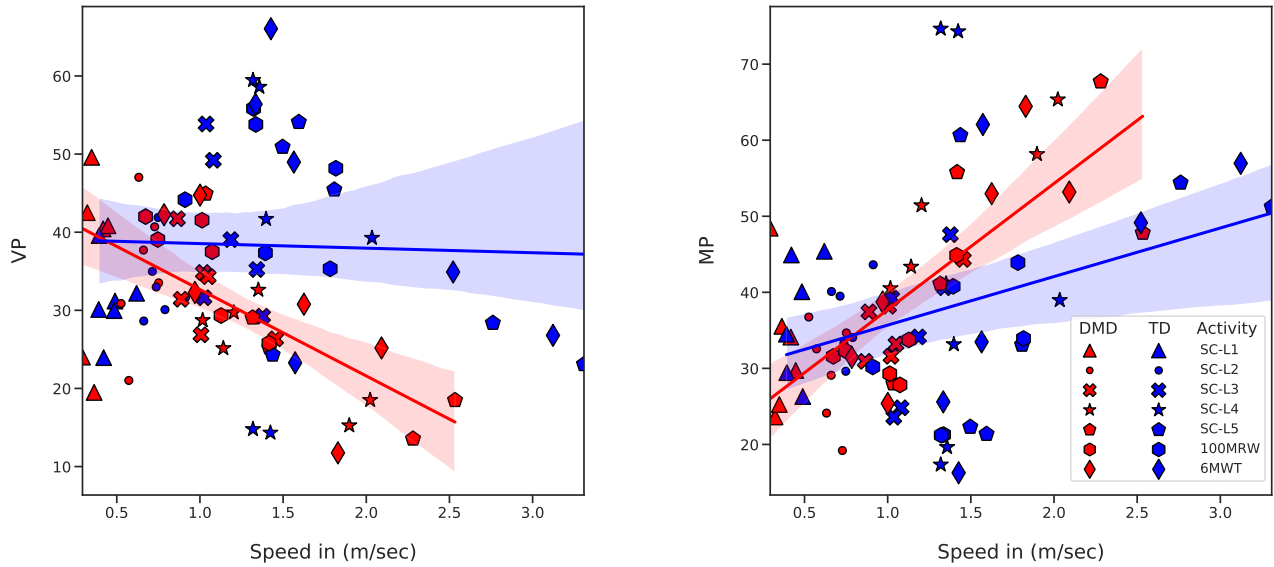
Table 3

This table presents a summary of the highest accuracy obtained by using three different methods: CML with Clinical Features (CML-CF), CML with raw data (CML-RAW), and DL with raw signal (DL-RAW). In the CML, the six different techniques were used are Random Forest (RF), Decision-Tree (DT), Support-Vector Machine (SVM), k-Nearest Neighbors (kNN), Gaussian Naive Bayes (GNB), Logistic Regression (LR). On the other hand, in DL, Convolutional neural networks (CNN) were used. In CML-RAW and DL-RAW, the Time-Window (TW) that obtains the highest accuracy was reported.

Activity	CML-CF				CML-RAW						DL-RAW	
	Alg.	CML (%)	PCA (%)	LDA (%)	TW-CML (Samples)	CML (%)	TW-PCA (Samples)	PCA (%)	TW-LDA (Samples)	LDA (%)	TW (Samples)	CNN (%)
SC-L1	RF	50.00	58.33	58.33	10,30,50,90,100	25.00	90	50.00	90	58.33	90,150	58.33
	DT	41.67	66.67	50.00	30	50.00	10,150	50.00	90	50.00		
	SVM	25.00	58.33	33.33	90,100,150	41.67	90,150	50.00	90,100	58.33		
	kNN	58.33	50.00	33.33	90,150	41.67	90	58.33	90	58.33		
	GNB	50.00	50.00	58.33	30,50,90,100,150	33.33	10,50,100,150	50.00	90	75.00		
	LR	33.33	66.67	58.33	150	50.00	150	50.00	90	58.33		
SC-L2	RF	50.00	33.33	58.33	30	41.67	10,30	50.00	100	58.33	90,150	83.33
	DT	66.67	50.00	58.33	100	58.33	100	50.00	100	58.33		
	SVM	41.67	8.33	58.33	90,100	41.67	10	50.00	150	66.67		
	kNN	50.00	33.33	58.33	10,30,90	41.67	10,30,50	50.00	100,150	58.33		
	GNB	50.00	25.00	58.33	10,30,50,100,150	58.33	100	50.00	30,90,100,150	50.00		
	LR	50.00	41.67	58.33	90	50.00	90,100	33.33	100	58.33		
SC-L3	RF	66.67	25.00	75.00	30,90	50.00	10	50.00	90	66.67	30,90	83.33
	DT	83.33	33.33	75.00	30	58.33	30,90	50.00	90	66.67		
	SVM	50.00	58.33	58.33	50,90	41.67	10	41.67	10,90	50.00		
	kNN	58.33	50.00	75.00	10,30,50,90,100,150	50.00	10,30,90	50.00	50,90	66.67		
	GNB	58.33	58.33	58.33	90,100,150	50.00	10,30	33.33	90	66.67		
	LR	58.33	66.67	75.00	50	66.67	100	33.33	90	66.67		
SC-L4	RF	50.00	41.67	66.67	150	41.67	150	41.67	100	58.33	100,150	91.67
	DT	58.33	66.67	66.67	100	75.00	100	50.00	100,150	66.67		
	SVM	66.67	75.00	50.00	50,100	50.00	100	41.67	100	58.33		
	kNN	58.33	58.33	50.00	30	58.33	150	58.33	100	66.67		
	GNB	75.00	41.67	58.33	50,90,100	58.33	100,150	58.33	100	66.67		
	LR	75.00	50.00	66.67	150	66.67	100,150	50.00	100	66.67		
SC-L5	RF	36.36	54.55	72.73	10,30,50,90,100,150	54.55	150	63.64	50	72.73	50	72.73
	DT	54.55	54.55	72.73	150	63.64	150	63.64	50	72.73		
	SVM	45.45	18.18	72.73	10,30,50,90,100,150	27.27	10,90,150	54.55	50	72.73		
	kNN	63.64	45.45	72.73	90	63.64	150	63.64	50	72.73		
	GNB	27.27	18.18	72.73	100,150	36.36	10,90,150	63.64	50	63.64		
	LR	90.91	18.18	72.73	100	63.64	150	63.64	50	72.73		
6MWT	RF	83.33	66.67	75.00	150	41.67	50,100	66.67	100,150	25.00	150	91.67
	DT	91.67	66.67	75.00	90	83.33	10	75.00	100	25.00		
	SVM	91.67	91.67	75.00	50,90,100,150	83.33	10	75.00	100	25.00		
	kNN	91.67	91.67	75.00	30,50	83.33	50,90	75.00	10,30,50	50.00		
	GNB	83.33	75.00	83.33	30,50,90,100,150	83.33	90,100	58.33	100	25.00		
	LR	83.33	83.33	75.00	100	25.00	10,30,50,90,100,150	0.00	100	25.00		
100MRW	RF	58.33	75.00	58.33	10	50.00	90	58.33	50	66.67	100	91.67
	DT	75.00	75.00	58.33	30,50	75.00	10,90,150	58.33	50	75.00		
	SVM	58.33	25.00	58.33	50,90,100,150	75.00	30,50,100,150	58.33	50,150	58.33		
	kNN	66.67	66.67	58.33	90	58.33	10,50,150	75.00	50,150	58.33		
	GNB	66.67	66.67	66.67	30,50,90,100,150	66.67	30,50,90,100	66.67	10,30,90	50.00		
	LR	83.33	66.67	58.33	50	75.00	10,30,50,90,100,150	50.00	50,150	58.33		

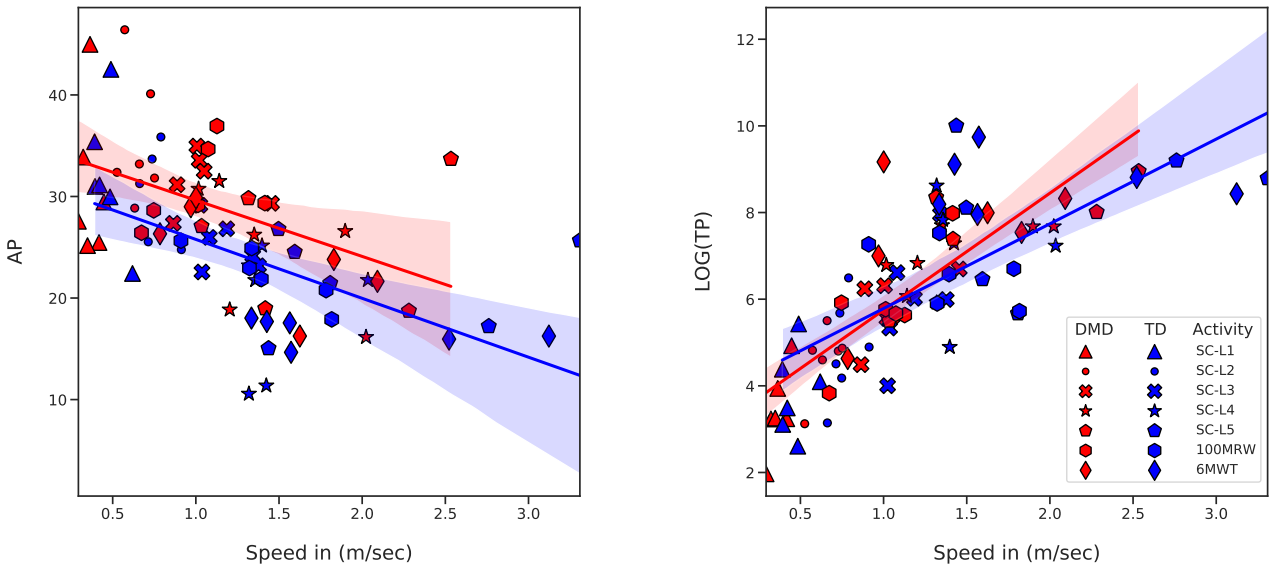
children, as total power increased with ambulatory velocity, approximately 40% of power on average was expended as vertical movement Fig-6(a). The percentage of mediolateral movement averaged from around 30% at a slow walk to nearly 50% at a running speed of greater than 3m/sec (Fig-6(b)). The average AP force began around 30% at a slow walk and decreased to approximately 15% at faster running speeds (Fig-6(c)). In boys with DMD, the percentage of power expended in vertical movement at slow walks was similar to TD controls at approximately 40% at slow walking speeds, but in contrast to TD controls dropped sharply to

20% or less at or above running speeds of 2m/sec ($p < 0.0001$) (Fig-6(a)). Percent mediolateral power was also similar to TD controls at lower walking speeds at approximately 25% of TP, but it increased at a more pronounced rate compared to TD controls reaching nearly 60% at running speeds ($p = 0.002$) (Fig-6(b)). The anteroposterior force was slightly elevated compared to TD controls but declined at a nearly identical rate as speed increases (Fig-6(c)). It is notable the significant differences between boys with DMD and TD controls in the overall difference between the percentage of vertical force and percentage of anteroposterior force at comfortable,



(a) Graph representing changes in axial percentages of VP with increasing speed in DMD and TD.

(b) Graph representing changes in axial percentages of MP with increasing speed in DMD and TD.



(c) Graph representing changes in axial percentages of AP with increasing speed in DMD and TD.

(d) The changes in log TP with increasing speed in DMD and TD.

Figure 6: Graph representing changes in axial percentages of powers with increasing speed in DMD and TD.

self selected walking to running speeds (Table-2).

3.4. Differentiation between DMD and TD Controls Using Artificial Intelligence Approaches

Three different AI approaches were performed: CML-CF, CML-RAW, and DL-RAW. Fig-7 and Table-3 is a summary of the best results obtained from each approach. This figure represents the optimal accuracy obtained by perform-

ing the seven different gait activities: SC-L1, SC-L2, SC-L3, SC-L4, SC-L5, 6MWT, 100MRW (described in Section 2.3). Leave-one-out cross-validation was used to verify the accuracy results. The implemented methods achieve the best accuracy of 91.67%. We also observed that activities that were performed at high speed (e.g., 6MWT, and 100MRW, SC-L4) have more differentiable patterns for the AI models than the activities that were performed with a slower speed

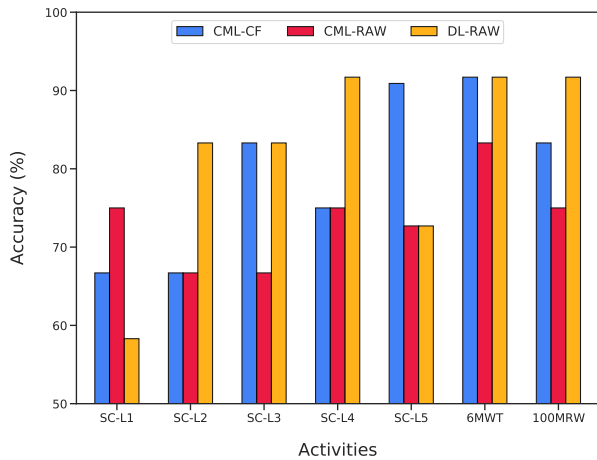


Figure 7: The optimal classifier's accuracy of CML-CF, CML-RAW, and DL-RAW. The y-axis represents the classifier accuracies, while the x-axis represents different activities. As can be seen, the classifier accuracy increases with speed.

(e.g., SC-L1, SC-L2, SC-L3).

3.4.1. CML-CF and CML-RAW Approaches

We evaluated CML algorithms using CFs (CML-CF, Fig-7) and raw data (CML-RAW, Fig-7). We report the best classifier's accuracy among 6 different CML techniques: RF, DT, SVM, kNN, GNB, and LR. For each feature type (clinical or raw), three different methods were used: no projection, PCA projection, and LDA projection. Each group of results represents one of seven different activities mentioned previously.

3.4.2. DL-RAW Approach

We evaluated a CNN (DL algorithm) on raw data (DL-RAW, Fig-7). Since DL algorithms require a large amount of data, we only evaluated raw signal-features. For raw data each activity was divided into fixed TWs to provide more data for the DL model. Table-3 reports the detailed results of DL-RAW analyses and optimization of TW segment length. Our model achieved the best accuracy of 91.67% with TW of 3.3 and 5 sec (100 and 150 samples) in high-speed activities (6MWT, 100MRW, and SC-L4), representing TWs that are large enough to include several complete gait cycles.

4. Discussion

The purpose of our study was to explore the utility and feasibility of collecting clinically meaningful gait data using consumer-level accelerometers outside of the formal gait laboratory setting, and to explore a range of classical and AI analytical methods to differentiate between children with DMD and TD controls of different ages. Extracting and describing a combination of well-known and understood temporospatial gait features allowed us to begin to identify some of the characteristics that CML and DL tools used to deter-

mine membership in DMD and TD control groups.

4.1. Extracted Gait Features are Consistent with Clinical Observations

It is commonly appreciated that in people with DMD, the temporospatial gait characteristics of speed, step frequency and step length are on average lower than in TD peers. However, in a recent review by Goudriann [12], the authors noted that several of the classical studies describing significant differences in walking speed, step frequency and step length between DMD boys and TD controls used data that was not normalized for height. In contrast, in the studies where height was used to normalize those features, only step length remained significantly different. We extracted gait feature data from signals derived from a single mobile phone-based tri-axial accelerometer using methods similar to those described by Barthelemy [3], and our data demonstrated that across a range of commonly-attained speeds, our extracted gait features differ between DMD and TD controls but only some differences reach statistical significance. Our observation that overall speed of ambulation and step frequency, when adjusted for height, did not differ significantly appears consistent with Goudriann's observations. Also, in agreement with earlier observations, our overall height adjusted step lengths were the only temporospatial feature that was significantly reduced in DMD boys. Analysis of power spectra of time-series gait data using single sensors during walking has been explored in comparison to some mobility-limited human populations, but has not to our knowledge been previously applied in a DMD population. The series of papers by Barthelemy [3] [2] using single sensors to measure gait characteristics of dystrophic GRMD dogs and to evaluate extracted clinical features using linear discriminant analysis methods demonstrated the utility of such methods and provided inspiration for our approach. When viewed together, patterns of increasing power with increasing velocity combined with overall age-related decreases in TD children suggest that we observe the development of a more efficient, adult-like gait. Our observation that patterns are not as clear in children with DMD could be because the progression of disease masks signals that otherwise be indicate gait maturation. The overall increased power with decreased vertical percent power and increased lateral power that we observed also appears consistent with clinical observations of the development of a more lateral, Trendelenburg gait pattern in children with DMD, and appears consistent with observations of increased step width in boys with DMD by D'Angelo [7] In typical individuals, as walking speed increases and progresses to running, ground clearance for the foot and leg in the swing phase is achieved through a gradual but proportional increase in vertical movement. In people with DMD with progressing weakness, swing phase leg clearance at increasing velocities is achieved through substitution using a more pronounced lateral shift of the center of mass to the stance phase leg with the elevation of the contralateral hip. This more lateral gait style is effective but also less efficient, and results in greater work for reduced forward motion as

demonstrated by prior studies showing increased heart rate-based energy expenditure of ambulation with increasing step frequency in DMD boys measured by COSMED portable metabolic testing combined with StepWatch activity monitoring [20].

4.2. Utility and Feasibility of CML and DL Approaches to Extracted Feature and Raw Data

We investigated two different AI techniques: CML and DL. We report the optimal outcome for each gait velocity Table-3. We also show that using AI with extracted CFs to predict membership in the DMD group yields satisfactory results, with correct predictions in over 90% of participants. Artificial intelligence approaches typically show improved accuracy with larger volumes and types of data, and we thus expect that identifying and extracting more correlated CFs will improve the current model's outcome in future studies. This improvement of the outcome depends on how these new CFs related to the gait cycle objectively and quantitatively. On the other hand, DL has been successfully proven to have a high accuracy in several medicine fields [22].

Nonetheless, DL requires a large amount of data to train. Furthermore, the drawback of using DL in the medical field is the lack of explainability, especially in the context of clinical trials where it is not favorable to use "black-box" models without an explanation of what differentiating characteristics are being used for classification. However, the promising results in DL with the CFs method should encourage researchers to transfer the knowledge yielded from DL to improve the existing CFs methods, and conversely to use CFs to aid in the interpretation of DL results.

4.3. CML with Dimensional Reduction

Using PCA and LDA provides a visual representation of the DMD and TD group's distribution. We reduce the dimensionality of the features to 2D using PCA and 1D using LDA. Both TD and DMD participant's features after PCA and LDA reduction tend to form different groups. LDA (supervised) maximizes the separability between classes, and PCA (unsupervised) maximizes the variance within the classes. Resulting visual representation of these group separation methods provides valuable feedback about model performance as well as a degree of difference between groups, even in the presence of complex, multi-dimensional data. When the separation is high, the distance between the groups becomes more obvious, and the two groups tend to be separable. This gives an indicator that the model would yield a high classification accuracy. On the other hand, when the two groups intersect which indicates high similarity between the two groups DMD and TD, the classifier yields low accuracy. In PCA (Table-3), we notice that the model's accuracy increases in the high-speed activities such as SC-L4 (fast walk) 100MRW, and 6MWT. We can see that while the accuracy of the original model (without dimensionality reduction) is always higher than both PCA and LDA, overall PCA performs better than LDA. Using LDA reduces the model accuracy sharply due

to the high intersection between the DMD and TD groups in 1D space. We observed, in 6MWT activity, the PCA reaches 91.67% which is the same accuracy as the original model while the LDA model's accuracy does not pass 83.33%. Therefore, PCA is more accurate as well as provides a helpful visual representation in high-speed activities which aids in a better understanding of the differences in gait patterns of the participants.

4.4. Utility of CML Models as Classifiers

CML without dimensionality reduction achieves high accuracy in the high-speed activities. For example, it achieves a maximum accuracy of 91.67% in the 6MWT. We believe the observation that speed and accuracy are correlated would encourage researchers to consider gait speed's effect on the gait characteristics. In this respect, CML approaches may be relying on elements of gait that are apparent to the eye, such as the observed differences in lateral movement or shortened relative step length that become more visually different with increasing gait speed. Our data demonstrate that CFs extracted from a single accelerometer worn during ambulation can provide information that is sufficient to identify disordered gait patterns using some of the CML methods.

4.5. Time Windowing of Raw Data to Capture Multiple Gait Cycles

We found that optimizing the TW to include multiple complete gait cycles improved model accuracy. By examining several TW sizes, we found that the optimal TW size should contain several complete gait cycles to improve classification accuracy. We conclude that a complete gait cycle is the smallest unit that could hold distinguishable gait pattern features. The model determines whether a TW is DMD or TD by capturing the unique gait patterns of the complete gait cycle among the DMD and TD groups. This allows us to simplify our methods and use ML/DL methods on minimally processed raw data in such a way that they are able to identify differences that we observe in clinical features, such as differences in step frequency and force, but in a manner that requires less expertise to extract clinical features. Having one or more gait cycles in each TW also helps the model to identify unique gait patterns in a TW. Using a small TW that captures an incomplete gait cycle could lead to an insufficient model that cannot capture gait patterns. On the other hand, using a large TW makes it difficult for the model to find the pattern since too much information exists in each TW. At different velocities, people with DMD and TD have similarities in some portion of their gait cycles, and even at faster velocities that are more difficult for people with DMD to achieve, some cycles may appear more typical than others. By examining the percentage of "typical/atypical" calls for each TW, it may be possible to use that percentage of typical to atypical gait cycles across a range of speeds to indicate the severity of disease at a given point in time and to track and quantify disease progress over time.

4.6. Evaluation of Raw Data Using CML and DL Models

AI models (supervised in our study) depend heavily on input features. When we apply CML approaches to raw accelerometer data (CML-RAW), the model achieves a maximum accuracy of 83.33%. While these numbers are lower than CML-CF, this method doesn't need any feature engineering effort. We believe a further investigation into improving the raw data as well as the algorithms could be a promising direction. Even though improving raw data in the AI models would lead to getting optimal results, it still suffers from a lack of clinical explainability. Therefore, when the clinical explanation is a major focus, it is favorable to extract clinical features that could be helpful to understand how the decisions are made in AI models. For DL-RAW methods accuracy increases with higher gait speeds. We found that there is a correlation between the group classification accuracy and the gait speed. The accuracy of DL-RAW models is very high in the activities with a higher speed, while the accuracy drops down when the speed is low Fig-7. Our results indicate that gait speed is an essential component in single accelerometer gait analysis [11], and that changes in gait speed can affect the gait characteristics and classification accuracy.

4.7. Effectiveness of CML and DL Models Differs Depending on Gait Velocity and Type of Gait

Using DL model with RAW data (DL-RAW) performs better than the other two methods with the exception of SC-L1 where CML with RAW data (CML-RAW) performs better, and SC-L5 where CML-CF performs better. Overall DL accuracy increases with speed of the activity, and since SC-L1 is the slowest speed activity, it performs poorly in this activity. The one exception to this comes from activity SC-L5, where participants run/walk as fast as possible but the DL-RAW only achieves 72.73%. This may be partially due to the fact that while not all participants are able to perform a typical double-off run, a DMD maximal effort "run" can also be a high-energy effort with similar forces on the accelerometer. Additionally, the running efforts on the 25-meter course are of short duration, which further reduces available training data. As we continue to collect data using our system, our modeling of running activities is likely to improve in accuracy. We see this in 100MRW where the duration of the activity is longer as it provides more data to the model and the model achieves a high accuracy despite the fact that only some participants run while others walk.

Study Limitations

The main limitation of this study is the small number of participants. Our current and future work aims to expand the scope of this experiment to a larger group of participants spanning multiple demographics and age groups. The effort is ongoing using the system we developed.

5. Conclusion

Use of low-cost consumer level mobile devices with single accelerometers to remotely measure differences in common clinical gait parameters represents an opportunity to expand the study of 3D gait analysis into the community setting. Our initial laboratory-based studies demonstrate ability to measure selected common temporospatial gait parameters across a range of typical ambulatory velocities in DMD and TD control children to detect significant differences in step length that are consistent with previous studies, as well as to detect differences in proportional power of accelerations in vertical, mediolateral and anteroposterior axes. By using these clinical gait parameters and raw data and employing both CML and DL models, we are able to correctly predict whether sensor data is derived from children with DMD 83.33% of the time at a comfortable walking pace, and over 91.67% of the time at a fast walk. By combining these approaches, we anticipate that through ongoing study we will be able to improve predictive accuracy and to identify additional clinically-useful parameters indicating typical growth and development, gait impairment and disease progression across a wide range of individuals with neuromuscular disease.

Funding Acknowledgement

This study was partially funded for participant assessment and data collection by grant from the U.S. Department of Defense (W81XWH-17-1-0477), and from a pilot grant from the University of California Center for Information Technology Research in the Interest of Society (CITRIS) and the Banatao Institute.

Acknowledgments

We thank Zainul Abi Din, Mohammad Newaz Sharif, Vehbi Esref Bayraktar, and Ammar Haydari for their diligent proofreading. We would also like to thank Erica Goude, and Omaid Sarwary for their assistance in the project management. We would like to thank all of our participants and families for donating their time to this project.

Declaration of Interest

The authors declare that they have no competing interests and no conflicts to declare.

CRedit Statement

Albara Ah Ramli, MS: Conceptualization, Methodology, Software, Formal analysis, Writing, Supervision, Validation, Investigation, Data Curation. Huanle Zhang, PhD: Writing - Review and Editing. Jiahui Hou, PhD: Writing - Review and Editing. Rex Liu, MS: Writing - Review and Editing. Xin Liu, PhD: Writing - Review and Editing, Methodology, Supervision. Alina Nicorici, BS: Investigation, Data Curation, Methodology. Daniel Aranki, PhD: Methodology, Software,

Formal analysis. Corey Owens, BS: Investigation, Data Curation. Poonam Prasad, BS: Investigation, Data Curation. Craig McDonald, MD: Conceptualization, Resources, Funding acquisition. Erik Henricson, PhD, MPH: Conceptualization, Methodology, Software, Formal analysis, Writing, Supervision, Funding acquisition, Investigation.

References

- [1] Alfano, L.N., Miller, N.F., Berry, K.M., Yin, H., Rolf, K.E., Flanagan, K.M., Mendell, J.R., Lowes, L.P., 2017. The 100-meter timed test: normative data in healthy males and comparative pilot outcome data for use in duchenne muscular dystrophy clinical trials. *Neuromuscular Disorders* 27, 452–457.
- [2] Barthélémy, I., Barrey, E., Aguilar, P., Uriarte, A., Chevoir, M., Thibaud, J.L., Voit, T., Blot, S., Hogrel, J.Y., 2011. Longitudinal ambulatory measurements of gait abnormality in dystrophin-deficient dogs. *BMC musculoskeletal disorders* 12, 75.
- [3] Barthélémy, I., Barrey, E., Thibaud, J.L., Uriarte, A., Voit, T., Blot, S., Hogrel, J.Y., 2009. Gait analysis using accelerometry in dystrophin-deficient dogs. *Neuromuscular Disorders* 19, 788–796.
- [4] Chen, S., Lach, J., Lo, B., Yang, G.Z., 2016. Toward pervasive gait analysis with wearable sensors: A systematic review. *IEEE journal of biomedical and health informatics* 20, 1521–1537.
- [5] Connolly, A.M., Florence, J.M., Craddock, M.M., Malkus, E.C., Schierbecker, J.R., Siener, C.A., Wulf, C.O., Anand, P., Golumbek, P.T., Zaidman, C.M., et al., 2013. Motor and cognitive assessment of infants and young boys with duchenne muscular dystrophy: results from the muscular dystrophy association dmd clinical research network. *Neuromuscular Disorders* 23, 529–539.
- [6] De Sanctis, R., Pane, M., Sivo, S., Ricotti, V., Baranello, G., Frosini, S., Mazzone, E., Bianco, F., Fanelli, L., Main, M., et al., 2015. Suitability of north star ambulatory assessment in young boys with duchenne muscular dystrophy. *Neuromuscular Disorders* 25, 14–18.
- [7] D'Angelo, M.G., Berti, M., Piccinini, L., Romei, M., Guglieri, M., Bonato, S., Degrate, A., Turconi, A.C., Bresolin, N., 2009. Gait pattern in duchenne muscular dystrophy. *Gait & posture* 29, 36–41.
- [8] Fowler, E.G., Staudt, L.A., Heberer, K.R., Sienko, S.E., Buckon, C.E., Bagley, A.M., Sussman, M.D., McDonald, C.M., 2018. Longitudinal community walking activity in duchenne muscular dystrophy. *Muscle & nerve* 57, 401–406.
- [9] Fraysse, B., Barthélémy, I., Qannari, E.M., Rouger, K., Thorin, C., Blot, S., Le Guiner, C., Chereil, Y., Hogrel, J.Y., 2017. Gait characterization in golden retriever muscular dystrophy dogs using linear discriminant analysis. *BMC Musculoskeletal Disorders* 18.
- [10] Ganea, R., Jeannot, P.Y., Paraschiv-Ionescu, A., Goemans, N.M., Piot, C., Van den Hauwe, M., Aminian, K., 2012. Gait assessment in children with duchenne muscular dystrophy during long-distance walking. *Journal of child neurology* 27, 30–38.
- [11] Gaudreault, N., Gravel, D., Nadeau, S., Houde, S., Gagnon, D., 2010. Gait patterns comparison of children with duchenne muscular dystrophy to those of control subjects considering the effect of gait velocity. *Gait & posture* 32, 342–347.
- [12] Goudriaan, M., Van den Hauwe, M., Dekeerle, J., Verhelst, L., Molenaers, G., Goemans, N., Desloovere, K., 2018. Gait deviations in duchenne muscular dystrophy—part 1. a systematic review. *Gait & posture* 62, 247–261.
- [13] Heberer, K., Fowler, E., Staudt, L., Sienko, S., Buckon, C.E., Bagley, A., Sison-Williamson, M., McDonald, C.M., Sussman, M.D., 2016. Hip kinetics during gait are clinically meaningful outcomes in young boys with duchenne muscular dystrophy. *Gait & posture* 48, 159–164.
- [14] Henmi, O., Shiba, Y., Saito, T., Tsuruta, H., Takeuchi, A., Shirataka, M., Obuchi, S., Kojima, M., Ikeda, N., 2009. Spectral analysis of gait variability of stride interval time series: comparison of young, elderly and parkinson's disease patients. *Journal of Physical Therapy Science* 21, 105–111.
- [15] Henricson, E., Aranki, D., Owens, C., Nicorici, A., Kurillo, G., McDonald, C., Bajcsy, R., 2019. A pilot study of a community-based gait monitor for children with duchenne muscular dystrophy. *Parent Project Muscular Dystrophy National Annual Conference*.
- [16] Jarchi, D., Pope, J., Lee, T.K., Tamjidi, L., Mirzaei, A., Sanei, S., 2018. A review on accelerometry-based gait analysis and emerging clinical applications. *IEEE reviews in biomedical engineering* 11, 177–194.
- [17] LeCun, Y., Bengio, Y., Hinton, G., 2015. Deep learning. *Nature* 521, 436–444.
- [18] Liu, R., Ramli, A.A., Zhang, H., Datta, E., Henricson, E., Liu, X., 2021. An overview of human activity recognition using wearable sensors: Healthcare and artificial intelligence. *arXiv preprint arXiv:2103.15990*.
- [19] McDonald, C.M., Henricson, E.K., Abresch, R.T., Florence, J.M., Eagle, M., Gappaier, E., Glanzman, A.M., Group, P.G..D.S., Spiegel, R., Barth, J., et al., 2013. The 6-minute walk test and other endpoints in duchenne muscular dystrophy: longitudinal natural history observations over 48 weeks from a multicenter study. *Muscle & nerve* 48, 343–356.
- [20] McDonald, C.M., Widman, L.M., Walsh, D.D., Walsh, S.A., Abresch, R.T., 2005. Use of step activity monitoring for continuous physical activity assessment in boys with duchenne muscular dystrophy. *Archives of physical medicine and rehabilitation* 86, 802–808.
- [21] Mignardot, J.B., Deschamps, T., Barrey, E., Auvinet, B., Berrut, G., Cornu, C., Constans, T., Dedecker, L., 2014. Gait disturbances as specific predictive markers of the first fall onset in elderly people: a two-year prospective observational study. *Frontiers in aging neuroscience* 6, 22.
- [22] Miotto, R., Wang, F., Wang, S., Jiang, X., Dudley, J.T., 2018. Deep learning for healthcare: review, opportunities and challenges. *Briefings in bioinformatics* 19, 1236–1246.
- [23] Ramli, A.A., Liu, R., Krishnamoorthy, R., Vishal, I.B., Wang, X., Tagkopoulos, I., Liu, X., 2020a. Bwcn: Blink to word, a real-time convolutional neural network approach, in: Song, W., Lee, K., Yan, Z., Zhang, L.J., Chen, H. (Eds.), *Internet of Things - ICIOT 2020*, Springer International Publishing, Cham. pp. 133–140.
- [24] Ramli, A.A., Liu, X., Henricson, E., . Walk4me system. <https://albara.ramli.net/research/walk4me/>.
- [25] Ramli, A.A., Nicorici, A., Prasad, P., Hou, J., McDonald, C., Liu, X., Henricson, E., 2020b. An automated system for early diagnosis, severity, and progression identification in duchenne muscular dystrophy: a machine learning and deep learning approach, in: *Annual Human Genomics Symposium – University of California Davis Medical Center*, pp. 12–12.
- [26] Shin, H., Roth, H.R., Gao, M., Lu, L., Xu, Z., Nogues, I., Yao, J., Mollura, D., Summers, R.M., 2016. Deep convolutional neural networks for computer-aided detection: Cnn architectures, dataset characteristics and transfer learning. *IEEE Transactions on Medical Imaging* 35, 1285–1298.
- [27] Staab, W., Hottowitz, R., Sohns, C., Sohns, J.M., Gilbert, F., Menke, J., Niklas, A., Lotz, J., 2014. Accelerometer and gyroscope based gait analysis using spectral analysis of patients with osteoarthritis of the knee. *Journal of physical therapy science* 26, 997–1002.
- [28] Sutherland, D.H., Olshen, R., Cooper, L., Wyatt, M., Leach, J., Mubarak, S., Schultz, P., 1981. The pathomechanics of gait in duchenne muscular dystrophy. *Developmental Medicine & Child Neurology* 23, 3–22.
- [29] Tanawongsuwan, R., Bobick, A., 2003. Performance analysis of time-distance gait parameters under different speeds, in: *International Conference on Audio-and Video-Based Biometric Person Authentication*, Springer. pp. 715–724.